

FINITE ELEMENT METHODS FOR ACTIVE PARTICLES IN FLUIDS

Stevens Paz Sánchez and Gustavo C. Buscaglia

Departamento de Matemática Aplicada e Estatística, Instituto de Ciências Matemáticas e de Computação (ICMC), Universidade de São Paulo, Campus de São Carlos, Caixa Postal 668, 13560-970 São Carlos, São Paulo, Brazil, espeisan@usp.br, gustavo.buscaglia@icmc.usp.br

Keywords: Finite element method, microparticles, fluid-solid interaction, squirmers.

Abstract. The dynamics of active microparticles, such as phoretic or biological squirmers, results from the imposition of velocities and/or surface forces at the interface of the fluid-solid interaction problem. This allows the squirmer, which could be a ciliated microorganism or a Janus particle for example, to attain net displacements in low Reynolds number regimes. This problem involves large geometrical deformations of the domain, since the rigid-body motions of each squirmer are unknowns of the problem. We present a finite element method that admits general interface conditions for these particles and, contrary to popular boundary-element methods, works for both linear and nonlinear rheological models. Numerical examples are presented showing the effect of nonlinearities in the fluid rheology and in the dependence of the tangential force with the slip velocity at the interface.

1 INTRODUCTION

The mathematical treatment of a *squirmers*, which is a model of a microswimmer consisting of a deformable body that swims via small shape oscillations, has mainly dealt with those of spherical shape, to which analytical or semi-analytical (i.e., series expansion) techniques can be applied (Lighthill, 1952; Blake, 1971; Pedley, 2016). Numerical approximations are needed to predict the motion of confined squirmers, of non-spherical squirmers, of squirmers interacting with other squirmers or other particles, etc. The most frequent technique in the literature is the boundary element method (Zhang et al., 2015; Ishimoto and Gaffney, 2017), which expresses the velocity field in terms of Stokeslets. Boundary element methods are attractive because only the squirmer's surface needs to be meshed, and there is little need of remeshing along the squirmers evolution.

Though finite element/volume methods certainly require efficient meshing strategies, they have some advantages to model squirmers that in many applications make them preferable. These methods readily deal with non-Newtonian rheology and non-zero Reynolds numbers, whereas boundary elements rely on the problem's linearity. Further, finite elements/volumes provide a sparse representation of the volumetric velocity field for advection computations, while boundary element results need to undergo a quite costly post-processing step.

Notwithstanding, finite element/volume methods for squirmers are quite absent in the literature. In this work we provide a formulation that turns a finite element Navier-Stokes (NS) solver into a squirmer simulator that contemplates particles of arbitrary shape and motion and allows general boundary conditions at the fluid-solid interface.

2 SQUIRMER KINEMATICS

A squirmer is modeled as a rigid body, for which all possible configurations are translations and rotations of a reference domain $\mathcal{B}^* \subset \mathbb{R}^d$. Taking an arbitrary point \mathbf{X}_c as center of rotation, at all times t there exists a point $\mathbf{x}_c(t)$ and a rotation matrix $\mathbf{Q}(t)$ such that the position $\mathbf{x}(\mathbf{X}, t)$ of the material point \mathbf{X} is given by $\mathbf{x}(\mathbf{X}, t) = \mathbf{x}_c(t) + \mathbf{Q}(t)(\mathbf{X} - \mathbf{X}_c)$.

Because $\mathbf{Q}(t)$ belongs to $\mathbf{SO}(d) = \{\mathbf{Q} \in \mathbb{R}^{d \times d} : \mathbf{Q}^{-1} = \mathbf{Q}^T, \det[\mathbf{Q}] = 1\}$, the manifold of possible configurations of the squirmer is $Q = \mathbb{R}^d \times \mathbf{SO}(d)$ and the body's Eulerian velocity \mathbf{u}_B is given by $\mathbf{u}_B(\mathbf{x}, t) = \mathbf{v}_c(t) + \boldsymbol{\omega}(t) \times (\mathbf{x} - \mathbf{x}_c(t)) = \mathbf{H}(\mathbf{q}(t), \mathbf{x}) \mathbf{s}(t)$, where $\mathbf{v}_c(t) = \dot{\mathbf{x}}_c(t)$ is the translational velocity and $\boldsymbol{\omega}(t)$ is the pseudovector of angular velocities in the spatial frame, which relates to $\mathbf{Q}(t)$ and $\dot{\mathbf{Q}}(t)$ by $\dot{\mathbf{Q}}\mathbf{Q}^T = \text{sk}[\boldsymbol{\omega}]$ where the isomorphism $\text{sk}[\cdot]$ between vectors and skew-symmetric matrices is the classic skew-symmetric operator. For $d = 2$ the generalized coordinates can be changed to $\mathbf{q}(t) = (\mathbf{x}_c(t), \theta(t))$, replacing the rotation matrix \mathbf{Q} by the rotation angle $\theta \in \mathbb{R}$ of which the time derivative $\omega = \dot{\theta}$ is the rotational velocity of the body. The velocity array is $\mathbf{s} = (\mathbf{v}_c, \boldsymbol{\omega})^T \in \mathbb{R}^{n_c}$, $n_c = d + \frac{d(d-1)}{2}$. If $d = 3$, \mathbf{s} relates to $\dot{\mathbf{q}} = (\mathbf{v}_c, \dot{\mathbf{Q}})$ through the operator $\text{sk}[\cdot]$. If $d = 2$ we simply have $\mathbf{s} = \dot{\mathbf{q}}$. The matrix $\mathbf{H}(\mathbf{q}(t), \mathbf{x}) \in \mathbb{R}^{d \times n_c}$, of which the first d columns (from pure translations) are the identity matrix \mathbf{I}_d and the next $n - d$ columns (from pure rotations) are $-\text{sk}[\mathbf{x} - \mathbf{x}_c(t)]$.

The ambient fluid is governed by the NS equations, $\rho \frac{D\mathbf{u}}{Dt} - \nabla \cdot \boldsymbol{\sigma} = \mathbf{0}$ and $\nabla \cdot \mathbf{u} = 0$ in $\Omega_f(t)$, $t \in (0, T)$, where ρ is the density, \mathbf{u} the Eulerian velocity field, D/Dt the material derivative and $\boldsymbol{\sigma}$ the Cauchy stress tensor. The fluid will be assumed quasi-Newtonian for simplicity, i.e., $\boldsymbol{\sigma} = -p\mathbf{I}_d + 2\mu\nabla^S\mathbf{u}$, where p is the pressure, μ is the (possibly shear-rate dependent) viscosity and $\nabla^S\mathbf{u} = \frac{1}{2}(\nabla\mathbf{u} + \nabla\mathbf{u}^T)$, but other rheological models can be considered.

3 THE FSI FORMULATION

The presence of the squirmer intervenes in two ways in the problem definition; through the geometry of the flow domain Ω_f , since $\Omega_f(t) = \Omega \setminus \mathcal{B}(t)$, and through the kinematical and dynamical compatibility conditions at $\partial\mathcal{B}(t)$. These are: a) *kinematical condition*, imposing the jump in velocity between the solid and the fluid to be zero in the normal direction (non-penetration condition) and some slip velocity \mathbf{u}_s in the tangential direction, so that $\mathbf{u}(\mathbf{x}, t) = \mathbf{u}_B(\mathbf{x}, t) + \mathbf{u}_s(\mathbf{x}, t)$, $\forall \mathbf{x} \in \partial\mathcal{B}(t)$, $\forall t$; b) *tangential force equilibrium*, in which the force \mathbf{f}_s exerted by the squirmer on the adjacent fluid satisfies $\mathbf{P}_\tau \boldsymbol{\sigma}(\mathbf{x}, t) \mathbf{n} = \mathbf{f}_s(\mathbf{x}, t)$, $\mathbf{x} \in \partial\mathcal{B}(t)$, $t \geq 0$, where $\mathbf{P}_\tau = \mathbf{I}_d - \mathbf{n} \mathbf{n}^T$ is the projection matrix onto the tangent plane to $\partial\mathcal{B}(t)$ at \mathbf{x} , with normal unit vector \mathbf{n} pointing into the body; and c) *global force and torque balance*, in which, neglecting the inertia of the squirmer, the total force and torque on it must be zero, that is, for all t , $\int_{\partial\mathcal{B}(t)} \boldsymbol{\sigma} \mathbf{n} dS = \mathbf{0}$, and $\int_{\partial\mathcal{B}(t)} (\mathbf{x} - \mathbf{x}_c) \times \boldsymbol{\sigma} \mathbf{n} dS = \mathbf{0}$.

Though *kinematical* and *tangential force* conditions must necessarily hold for the solution to be physically meaningful, the two quantities \mathbf{u}_s and \mathbf{f}_s cannot be simultaneously imposed as data of the problem in the same region.

Here we will just detail the case in which the tangential slip velocity is known, this is, we are given a vector field $\mathbf{u}_s^*(\mathbf{X}, t)$ in the material frame, such that

$$\mathbf{u}_s(\mathbf{x}, t) = \mathbf{u}_s(\mathbf{x}(\mathbf{X}, t), t) = \mathbf{Q}(t) \mathbf{u}_s^*(\mathbf{X}, t), \quad \mathbf{X} \in \partial\mathcal{B}^*.$$

The mathematical problem reads as follows: Given $\mathbf{q}(t = 0)$ and $\mathbf{u}(\mathbf{x}, t = 0)$ (this latter datum is only needed if $\rho > 0$), determine $\mathbf{q}(t) = (\mathbf{x}_c(t), \mathbf{Q}(t))$, $\mathbf{s}(t) = (\mathbf{v}_c(t), \boldsymbol{\omega}(t))$, $\mathbf{u}(\mathbf{x}, t)$ and $p(\mathbf{x}, t)$ for $0 < t \leq T$ and $\mathbf{x} \in \Omega_f(t)$ satisfying

$$\frac{d\mathbf{x}_c}{dt} = \mathbf{v}_c, \tag{1}$$

$$\frac{d\mathbf{Q}}{dt} = \text{sk}[\boldsymbol{\omega}] \mathbf{Q}, \tag{2}$$

$$\mathbf{u}(\mathbf{x}, t) - \mathbf{H}(\mathbf{q}(t), \mathbf{x}) \mathbf{s}(t) = \mathbf{u}_s(\mathbf{x}, t), \quad \text{on } \partial\mathcal{B}(t), \tag{3}$$

$$\rho \frac{D\mathbf{u}}{Dt} - 2\nabla \cdot (\mu \nabla^S \mathbf{u}) + \nabla p = \mathbf{0}, \quad \text{in } \Omega_f(t), \tag{4}$$

$$\nabla \cdot \mathbf{u} = 0, \quad \text{in } \Omega_f(t), \tag{5}$$

$$\int_{\partial\mathcal{B}(t)} \boldsymbol{\sigma} \mathbf{n} dS = \mathbf{0}, \tag{6}$$

$$\int_{\partial\mathcal{B}(t)} (\mathbf{x} - \mathbf{x}_c) \times \boldsymbol{\sigma} \mathbf{n} dS = \mathbf{0}. \tag{7}$$

Considering for interpretation purposes $\rho = 0$, we see that the main equations to be solved are (1)-(2), of which the right-hand side contains the *unique* values of $\mathbf{s} = (\mathbf{v}_c, \boldsymbol{\omega})$ that introduced in (3) impose velocity boundary conditions for the Navier-Stokes equations (4)-(5) that produce a force-free and torque-free solution. Notice that $\mathbf{q} = (\mathbf{x}_c, \mathbf{Q})$ intervenes in (3)-(7) not just explicitly (in (3)) but also through the geometry (i.e., $\Omega_f, \partial\mathcal{B}$). The problem clearly belongs to the class of fluid-solid-interaction ones, with negligible inertia in the solid.

The variational problem is formulated on the function space (Glowinski et al., 2001)

$$W(\mathbf{q}) = \left\{ \mathbf{w} \in H^1(\Omega_f(\mathbf{q}))^d : \mathbf{w} = \mathbf{0} \text{ on } \partial\Omega, \mathbf{w} = \mathbf{H}(\mathbf{q})\mathbf{d} \text{ on } \partial\mathcal{B}, \mathbf{d} \in \mathbb{R}^{n_c} \right\},$$

that can be decomposed as

$$W(\mathbf{q}) = W_0(\mathbf{q}) \oplus V(\mathbf{q}),$$

where $V(\mathbf{q})$ is the finite-dimensional space (of dimension n_c) of extensions of rigid-body motions, i.e.,

$$V(\mathbf{q}) = \{\mathbf{w} \in H^1(\Omega_f(\mathbf{q}))^d : \mathbf{w} = \mathcal{E} \mathbf{H}(\mathbf{q}) \mathbf{d}, \mathbf{d} \in \mathbb{R}^{n_c}\}$$

and $W_0 = H^1(\Omega_f(\mathbf{q}))^d$.

Above, \mathcal{E} is an extension (or lifting) linear operator that, given a (regular enough) function f defined on $\partial\mathcal{B}$, assigns to it $\mathcal{E}f \in H^1(\Omega_f)$ that coincides with f on $\partial\mathcal{B}$ and is zero on $\partial\Omega$. The action of this operator on vector or matrix fields defined on $\partial\mathcal{B}$ is defined by applying \mathcal{E} componentwise. Also, $\mathbf{H}(\mathbf{q}) \mathbf{d}$ is the vector field defined on $\partial\mathcal{B}$ by $[\mathbf{H}(\mathbf{q}) \mathbf{d}](\mathbf{x}) = \mathbf{H}(\mathbf{q}, \mathbf{x}) \mathbf{d}$. The matrix field $\tilde{\mathbf{H}}(\mathbf{q}) = \mathcal{E}\mathbf{H}(\mathbf{q})$ plays an important role in the picture.

The weak formulation of (3)-(7) takes the form: Find $(\mathbf{s}(t), \mathbf{u}, p)$, where \mathbf{u} must belong to $\mathcal{E}\mathbf{u}_s + \tilde{\mathbf{H}}(\mathbf{q}(t)) \mathbf{s}(t) + W_0(\mathbf{q}(t))$ and p must belong to $L_0^2(\Omega_f(t))$, such that

$$\begin{aligned} \int_{\Omega_f(t)} \rho \frac{D\mathbf{u}}{Dt}(\mathbf{x}, t) \cdot \mathbf{w}(\mathbf{x}) \, d\mathbf{x} + \int_{\Omega_f(t)} \boldsymbol{\sigma}(\mathbf{x}, t) : \nabla^S \mathbf{w}(\mathbf{x}) \, d\mathbf{x} &= 0, \\ \int_{\Omega_f(t)} z(\mathbf{x}) \nabla \cdot \mathbf{u}(\mathbf{x}, t) \, d\mathbf{x} &= 0, \end{aligned}$$

for all $(\mathbf{w}, z) \in W(\mathbf{q}(t)) \times L_0^2(\Omega_f(t))$.

4 NUMERICAL METHOD

4.1 Discretization

For each $t \in [0, T]$, $T > 0$, let $\mathcal{T}_h(t)$ be a triangulation of $\Omega_f(t)$, this is, a regular partition of the physical domain into non-empty compact subdomains, or elements, $\Omega^e(t)$ of characteristic size h , which define a discrete domain $\bar{\Omega}_{fh}(t) = \bigcup_e \Omega^e(t) \subset \bar{\Omega}(t)$. We assume for simplicity that Ω is polygonal and thus $\partial\Omega$ is exactly approximated. The interpolated boundary of the squirmer is denoted by $\partial\mathcal{B}_h(t)$, so that $\partial\Omega_{fh}(t) = \partial\Omega \cup \partial\mathcal{B}_h(t)$.

The fluid velocity \mathbf{u} and pressure p are approximated as

$$\mathbf{u}_h(\mathbf{x}, t) = \sum_{j \in \eta^U} \mathcal{N}^j(\mathbf{x}, t) \mathbf{u}^j(t), \quad p_h(\mathbf{x}, t) = \sum_{k \in \eta^P} \mathcal{M}^k(\mathbf{x}, t) p^k(t),$$

for $\mathbf{x} \in \bar{\Omega}_{fh}(t)$, in finite dimensional subspaces $U_h(t) \subset H^1(\Omega_f(t))^d$ and $M_h(t) \subset L_0^2(\Omega_f(t))$. The shape functions $\mathcal{N}^j(\cdot, t)$, $\mathcal{M}^k(\cdot, t)$ satisfy the nodal value property, namely,

$$\mathcal{N}^j(\mathbf{x}^i(t), t) = \begin{cases} 1, & \text{if } i = j \\ 0, & \text{if } i \neq j \end{cases},$$

where $\mathbf{x}^i(t)$ is the position of node i of the mesh $\mathcal{T}_h(t)$, for i belonging to the velocity global index set η^U . In particular, $\mathbf{u}_h(\mathbf{x}^i, t) = \mathbf{u}^i(t)$, for all $i \in \eta^U$. Similarly, $\mathcal{M}^k(\mathbf{x}^l(t), t) = \delta_{kl}$, so that $p_h(\mathbf{x}^l(t), t) = p^l(t)$ for pressure nodes \mathbf{x}^l indexed by the set η^P .

Assuming the mesh to have no hanging nodes, the interpolation space for the velocity is

$$U_h(\mathbf{q}) = \left\{ \mathbf{w} \in H^1(\Omega_{fh}(\mathbf{q}))^d : \mathbf{w}|_{\Omega^e} \in P_m(\Omega^e)^d, \text{ for all } e, \mathbf{w}|_{\partial\Omega} = \mathbf{0} \right\},$$

and for the pressure

$$M_h(\mathbf{q}) = \left\{ q \in L_0^2(\Omega_{fh}(\mathbf{q})) : q|_{\Omega^e} \in P_m(\Omega^e), \text{ for all } e \right\},$$

where $P_m(\Omega^e)$ is the space of polynomials in Ω^e of degree less than or equal to m . In particular, we consider a stabilized P_1/P_1 element (Hughes et al., 1989), though a Galerkin P_2/P_1 element was also successfully tested (Taylor and Hood, 1973).

4.2 Semidiscrete formulation

Let us introduce the following spaces

$$W_h(\mathbf{q}) = \left\{ \mathbf{w}_h \in U_h(\mathbf{q}) : \mathbf{w}_h = \mathbf{0} \text{ on } \partial\Omega, \mathbf{w}_h = \mathbf{H}(\mathbf{q})\mathbf{d} \text{ on } \partial\mathcal{B}_h, \mathbf{d} \in \mathbb{R}^{n_c} \right\}$$

$$W_{0h}(\mathbf{q}) = \left\{ \mathbf{w}_h \in U_h(\mathbf{q}) : \mathbf{w}_h = \mathbf{0} \text{ on } \partial\Omega, \mathbf{w}_h = \mathbf{0} \text{ on } \partial\mathcal{B}_h \right\}.$$

Further, for each time t , let the extension operator \mathcal{E} be the simplest and most popular one: If η_∂^U is the subset of η^U containing the indices of velocity nodes in $\partial\mathcal{B}_h$ and f is a continuous (piecewise P_m) function defined on $\partial\mathcal{B}_h$,

$$\mathcal{E}f = \sum_{i \in \eta_\partial^U} f(\mathbf{x}^i) \mathcal{N}^i(\mathbf{x}).$$

In other words, f is extended to Ω_{fh} by setting all nodal values not belonging to $\partial\mathcal{B}_h$ to zero and interpolating according to the adopted finite element space.

Since $U_h(\mathbf{q})$ restricted to $\partial\mathcal{B}_h$ contains at least P_1 polynomials, $\mathbf{w}_h = \mathbf{H}(\mathbf{q})\mathbf{d}$ is satisfied exactly for all \mathbf{d} . Up to the geometrical difference between $\partial\mathcal{B}$ and $\partial\mathcal{B}_h$, which is out of the scope of this contribution, it thus holds that

$$W_h(\mathbf{q}) \subset W(\mathbf{q}), \tag{8}$$

$$W_{0h}(\mathbf{q}) \subset W_0(\mathbf{q}), \tag{9}$$

$$W_h(\mathbf{q}) = W_{0h}(\mathbf{q}) \oplus V(\mathbf{q}). \tag{10}$$

Let \mathbf{u}_{sh} be the interpolant of \mathbf{u}_s in U_h (restricted to $\partial\mathcal{B}_h$). The configuration manifold $Q = \mathbb{R}^d \times \mathbf{SO}(d)$ is kept exact, but of course in the semidiscrete problem one computes approximations of the exact functions $\mathbf{q}(t) = (\mathbf{x}_c(t), \mathbf{Q}(t)) : [0, T] \rightarrow Q$ and $\mathbf{s}(t) = (\mathbf{v}_c(t), \boldsymbol{\omega}(t)) : [0, T] \rightarrow \mathbb{R}^{n_c}$. We add the subscript h to these functions to make this fact explicit.

The approximate velocity $\mathbf{u}_h(\cdot, t)$ is sought belonging to $W_h(\mathbf{q}_h(t))$ and satisfying (3). Thus, from (10), it can be decomposed as

$$\mathbf{u}_h = \tilde{\mathbf{H}}\mathbf{s}_h + \mathbf{u}_{0h} + \mathcal{E}\mathbf{u}_{sh},$$

where $\mathbf{u}_{0h} \in W_{0h}(\mathbf{q}_h(t))$. Let $\mathbf{H}^j(\mathbf{q}) = \tilde{\mathbf{H}}(\mathbf{q}, \mathbf{x}^j)$ (i.e., $\mathbf{H}^j(\mathbf{q}) = \mathbf{H}(\mathbf{q}, \mathbf{x}^j)$ if $j \in \eta_\partial^U$, and = $\mathbf{0}$, the null $d \times n_c$ matrix, otherwise). Then the nodal values $\mathbf{u}^j(t)$ of $\mathbf{u}_h(\cdot, t)$ are unconstrained unknowns if $j \in \eta_0^U$ (interior nodes, i.e., $\eta_0^U = \eta^U \setminus \eta_\partial^U$) and, for $j \in \eta_\partial^U$, they obey

$$\mathbf{u}^j(t) = \mathbf{H}^j(\mathbf{q}_h(t))\mathbf{s}_h(t) + \mathbf{u}_s^j(t),$$

where $\mathbf{u}_s^j = \mathbf{u}_s(\mathbf{x}^j(t), t)$.

The semidiscrete formulation then reads: *Determine functions $\mathbf{q}_h(t) = (\mathbf{x}_{ch}(t), \mathbf{Q}_h(t)) : [0, T] \rightarrow Q$, $\mathbf{s}_h(t) = (\mathbf{v}_{ch}(t), \boldsymbol{\omega}_h(t)) : [0, T] \rightarrow \mathbb{R}^{n_c}$, $\mathbf{u}_h(\cdot, t) \in W_h(\mathbf{q}_h(t))$ and $p_h(\cdot, t) \in M_h(\mathbf{q}_h(t))$ such that*

$$\mathbf{u}_h(\cdot, t) - \tilde{\mathbf{H}}(\cdot, t)\mathbf{s}_h(t) - \mathcal{E}\mathbf{u}_{sh}(\cdot, t) \in W_{0h}(\mathbf{q}_h(t)) \tag{11}$$

and

$$\frac{d\mathbf{x}_{ch}}{dt} - \mathbf{v}_{ch} = \mathbf{0}, \quad (12)$$

$$\frac{d\mathbf{Q}_h}{dt} - \text{sk}[\boldsymbol{\omega}_h] \mathbf{Q}_h = \mathbf{0}, \quad (13)$$

$$\int_{\Omega_{fh}} \rho \frac{D\mathbf{u}_h}{Dt} \cdot \mathbf{w}_h d\mathbf{x} + \int_{\Omega_{fh}} 2\mu(\nabla^S \mathbf{u}_h) \nabla^S \mathbf{u}_h : \nabla^S \mathbf{w}_h d\mathbf{x} - \int_{\Omega_{fh}} p_h \nabla \cdot \mathbf{w}_h d\mathbf{x} \\ \int_{\Omega_{fh}} \left[\delta_h \nabla \cdot \mathbf{u}_h \nabla \cdot \mathbf{w}_h + \tau_h \left(\rho \frac{D\mathbf{u}_h}{Dt} + \nabla p_h \right) \cdot [(\mathbf{u}_h - \mathbf{m}_h) \cdot \nabla] \mathbf{w}_h \right] d\mathbf{x} = 0, \quad (14)$$

$$\int_{\Omega_{fh}} z_h \nabla \cdot \mathbf{u}_h d\mathbf{x} + \int_{\Omega_{fh}} \frac{\tau_h}{\rho} \left(\rho \frac{D\mathbf{u}_h}{Dt} + \nabla p_h \right) \cdot \nabla z_h d\mathbf{x} = 0, \quad (15)$$

for all $\mathbf{w}_h \in W_h(\mathbf{q}_h(t))$, for all $z_h \in M_h(\mathbf{q}_h(t))$, for all t . The parameters τ_h and δ_h are introduced for stabilization and are assigned customary values, while \mathbf{m}_h is the mesh velocity as needed in any ALE formulation.

4.3 Time marching

In microscopic squirmers inertia is generally negligible. Dropping the inertia terms and expressing (11)-(15) in terms of the unknown arrays, one arrives at a differential-algebraic equation (DAE) that can be written as

$$\frac{d\mathbf{q}}{dt} = \mathbf{g}(\mathbf{q}, \mathbf{s}), \quad \mathbb{C}(\mathbf{q}, \underline{U}) \begin{pmatrix} \mathbf{s} \\ \underline{U} \\ \underline{P} \end{pmatrix} = \underline{Z}(\mathbf{q}). \quad (16)$$

with initial condition $\mathbf{q}(t=0) = \mathbf{q}_0$, where \underline{U} and \underline{P} are the nodal values of the fluid velocity and pressure, respectively. The matrix \mathbb{C} depends on \underline{U} through the rheological nonlinearity. Notice, on the other hand, that the dependence of \mathbb{C} and \underline{Z} on \mathbf{q} is quite involved. Every time \mathbf{q} is updated, the coordinates of the body and thus of the nodes on its surface change according to the kinematics of the system. This change is then extended to the interior nodes by some smoothing algorithm, which complicates the dependence further (Montefusco et al., 2014). This been said, any convergent scheme for DAEs could be used for (16).

5 APPLICATIONS

5.1 Squirmer in a Non-newtonian ambient fluid

We consider an axisymmetric spherical rigid squirmer of radius $R = 1$, with imposed slip velocity $\mathbf{u}_s = u_s \boldsymbol{\tau}_b$, where

$$u_s = B_1 \sin \vartheta + B_2 \sin \vartheta \cos \vartheta, \quad (17)$$

$B_1 = 3$, $B_2 = 1$, being $\vartheta \in [0, \pi]$ the polar coordinate measured from the direction of locomotion, $\mathbf{n}_b = (\sin \vartheta, \cos \vartheta)$ the exterior normal vector and $\boldsymbol{\tau}_b = (\cos \vartheta, -\sin \vartheta)$ the polar tangent vector. This swimmer is known as a *puller* squirmer (Pedley, 2016) characterized by the formation of a recirculation region behind it, due to the change of sign of u_s for some $\vartheta \in (0, \pi)$. In the inertialess newtonian case the exact swimming speed is $v_c = \frac{2}{3}B_1$.

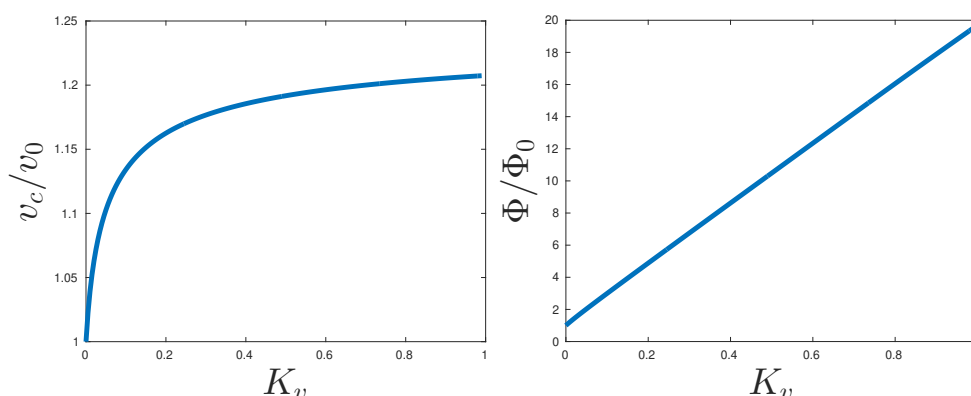


Figure 1: Translational speed (left) and viscous dissipation (right) of a spherical squirmer in a Non-newtonian fluid, normalized with those of the Newtonian case, as functions of K_v (see Equation 18).

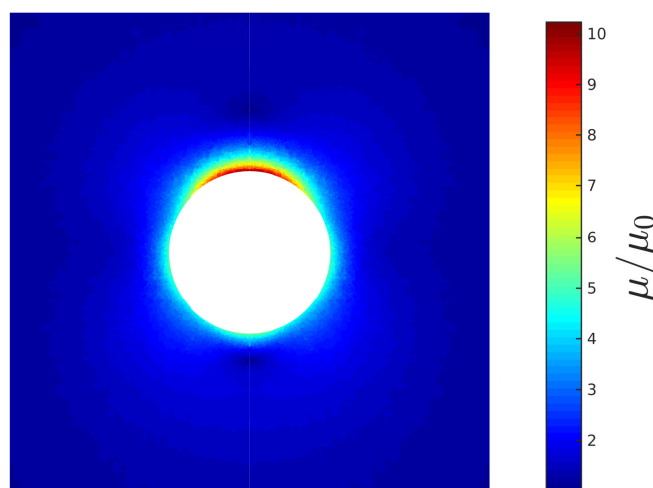


Figure 2: Fluid viscosity for $K_v = 1$.

Our squirmer is immersed in a shear-thickening fluid, for which we adopt the simple viscosity law

$$\mu = \mu_0 + K_v \|\nabla^S \mathbf{u}\|, \tag{18}$$

satisfying the condition $10^{-2} \leq \mu \leq 10^2$. The numerical results are shown in Figure 1 for the translational speed and viscous dissipation,

$$\Phi = \int_{\Omega_{fh}} 2\mu \nabla^S \mathbf{u} : \nabla^S \mathbf{u} dV,$$

as functions of K_v , in Figure 2 for the effective viscosity that develops around the squirmer, and in Figure 3 for the streamlines in the laboratory and particle frames. Finally, Figure 4 presents the velocity magnitude for $K_v = 0$ and $K_v = 100$.

5.2 A squirmer with nonlinear tangent force

It is reasonable to think that the slip velocity \mathbf{u}_s that the squirmer imposes on the adjacent fluid cannot be the same irrespective of the local force \mathbf{f}_s needed to sustain it. In fact, the

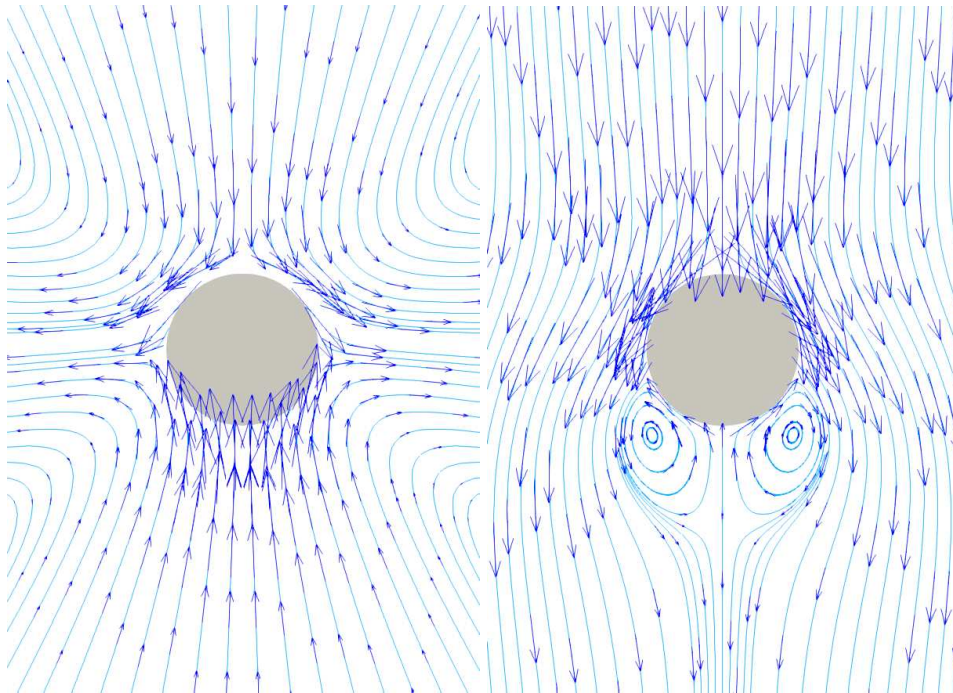


Figure 3: Numerically-obtained streamlines (light blue) and some velocity vectors (dark blue) in the laboratory frame (left) and in a frame moving with the particle (right) of a *puller* in a fluid with $K_v = 1$.

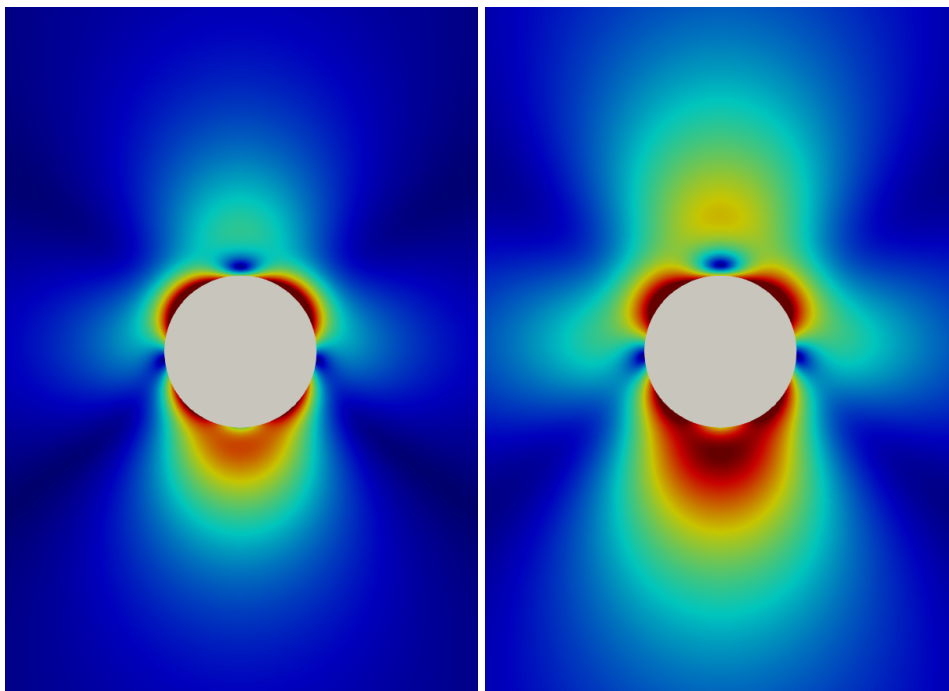


Figure 4: Fluid velocity magnitude for $K_v = 0$ (left) and $K_v = 1$ (right). Colors going from red to blue indicate maximum to minimum velocity magnitude.

local power spent by the squirmer is given by $\mathbf{f}_s \cdot \mathbf{u}_s$, which cannot be unbounded for physical realizability. In this paragraph we assess the proposed algorithm when the tangential force is

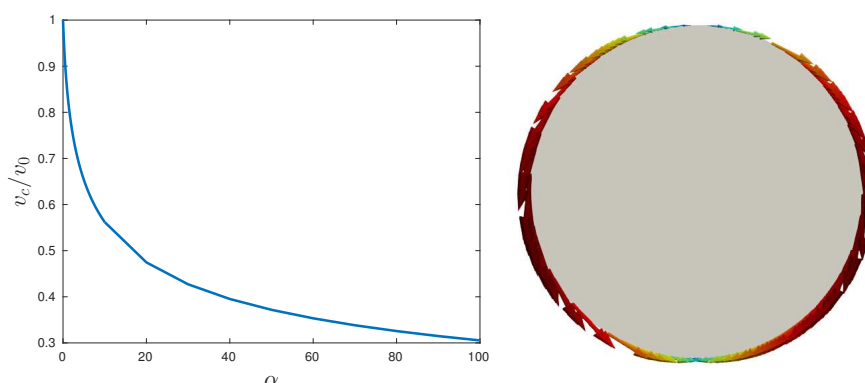


Figure 5: Translational speed as a function of the parameter α , relative to the value at $\alpha = 0$ (left). Slip velocity obtained from the nonlinear case when $\alpha = 100$ (right).

given by

$$\mathbf{f}_s(u_s) = \frac{1}{1 + \alpha u_s^2} \boldsymbol{\tau}_b$$

with $\alpha \geq 0$. Though the fluid is assumed Newtonian, this boundary condition induces a non-linear problem in which the slip velocity is no longer a datum. The variational formulation addressing the imposition of this tangential force, described in Paz Sánchez and Buscaglia (2019), requires to add to (14) the contribution of \mathbf{f}_s in the tangent direction while, in the normal direction, the non-penetration condition remains.

The effect of \mathbf{f}_s on the squirmer's speed v_c can be noticed when we increase the value of α . As shown in Figure 5, the squirmer's speed decreases quite sharply with α up to $\alpha \simeq 10$, where it is about 55% of the value corresponding to $\alpha = 0$. For larger values of α the reduction is less significant, being of 70% when $\alpha = 100$. In the same figure the slip velocity obtained for $\alpha = 100$ is also shown, corresponding to upwards motion. The streamlines, for this case, are presented in Figure 6 in both laboratory and moving frames, which resemble the ones of a *neutral* squirmer (i.e., a squirmer with $B_2 = 0$ in (17), see Paz Sánchez and Buscaglia (2019) and Pedley (2016)).

6 CONCLUSIONS

The mathematical setting and a numerical approximation suitable for the simulation of squirmers swimming through an ambient incompressible fluid have been presented. The formulation relies on finite elements but it can be easily adapted to other discretization schemes such as finite volumes. The technique applies straightforwardly to squirmers of any shape, contemplates inertial or rheological nonlinearities, and can handle interactions of any number of simultaneous squirmers in domains of arbitrary geometry. This was illustrated by a couple of simplified (one-dimensional) examples.

ACKNOWLEDGEMENTS

The authors gratefully acknowledge the financial support from São Paulo Research Foundation (FAPESP) (Grants #2014/14720-8, #2013/07375-0, #2018/08752-5) and from the Brazilian National Council for Scientific and Technological Development (CNPq) (Grants #305599/2017-8).

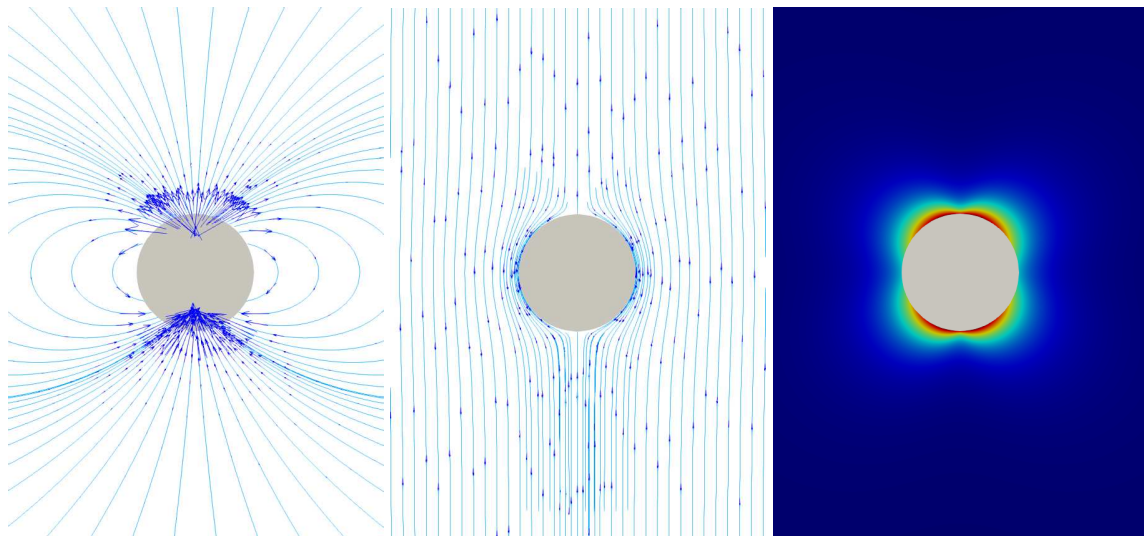


Figure 6: Numerically-obtained streamlines (light blue) and some velocity vectors (dark blue) in the laboratory frame (left) and in a frame moving with the particle (center) of a squirmer with nonlinear surface force f_s taking $\alpha = 100$. Contours of velocity magnitude (right).

REFERENCES

- Blake J. A spherical envelope approach to ciliary propulsion. *Journal of Fluid Mechanics*, 46(1):199–208, 1971.
- Glowinski R., Pan T., Hesla T., Joseph D., and Periaux J. A fictitious domain approach to the direct numerical simulation of incompressible viscous flow past moving rigid bodies: application to particulate flow. *Journal of Computational Physics*, 169(2):363–426, 2001.
- Hughes T.J., Franca L.P., and Hulbert G.M. A new finite element formulation for computational fluid dynamics: Viii. the galerkin/least-squares method for advective-diffusive equations. *Computer methods in applied mechanics and engineering*, 73(2):173–189, 1989.
- Ishimoto K. and Gaffney E.A. Boundary element methods for particles and microswimmers in a linear viscoelastic fluid. *Journal of Fluid Mechanics*, 831:228–251, 2017.
- Lighthill M. On the squirring motion of nearly spherical deformable bodies through liquids at very small reynolds numbers. *Communications on Pure and Applied Mathematics*, 5(2):109–118, 1952.
- Montefusco F., Sousa F.S., and Buscaglia G.C. High-order ALE schemes for incompressible capillary flows. *Journal of Computational Physics*, 278:133–147, 2014.
- Paz Sánchez S. and Buscaglia G.C. Simulating squirmers with volumetric solvers. *arXiv preprint arXiv:1903.07753*, 2019.
- Pedley T. Spherical squirmers: models for swimming micro-organisms. *IMA Journal of Applied Mathematics*, 81(3):488–521, 2016.
- Taylor C. and Hood P. A numerical solution of the Navier-Stokes equations using the finite element technique. *Computers & Fluids*, 1(1):73–100, 1973.
- Zhang P., Jana S., Giarra M., Vlachos P., and Jung S. Paramecia swimming in viscous flow. *The European Physical Journal Special Topics*, 224(17-18):3199–3210, 2015.